Optical orientation of acceptor-bound hole magnetic polarons in bulk (Cd,Mn)Te

E. A. Zhukov,[1,2] Yu. G. Kusrayev,[2] E. Kirstein,[1] A. Thomann,[1] M. Salewski,[1] N. V. Kozyrev,[2]
D. R. Yakovlev,[1,2] and M. Bayer[1,2]

[1]*Experimentelle Physik 2, Technische Universität Dortmund, D-44221 Dortmund, Germany*
[2]*Ioffe Institute, Russian Academy of Sciences, 194021 St. Petersburg, Russia*

The optically induced long-lived spin polarization in the bulk diluted magnetic semiconductor (Cd,Mn)Te with small manganese concentration is studied by picosecond pump-probe Kerr rotation. At temperatures below 6 K and in transversal magnetic field the Kerr rotation signal contains three components: two oscillating components, corresponding to the Larmor precession of manganese spins and spins of photoexcited electrons, and a long-lived (up to 15 ns) nonoscillating component. The latter one is provided by optical orientation of equilibrium hole magnetic polarons involving holes bound to acceptors. The origin of the anisotropy controlling the orientation and the spin dynamics of the acceptor-bound hole magnetic polaron in bulk (Cd,Mn)Te is discussed.

I. INTRODUCTION

One of the main tasks of spintronics is search and investigation of spin systems providing fast switching and long-lived memory, which may be used for quantum information technologies [1,2]. For that, diluted magnetic semiconductors (DMS) containing localized spins of magnetic ions, like Mn, Cr, or Fe, are often used as model systems [3]. Optical orientation of the localized spins is possible via the spin-polarized carriers photogenerated by circularly polarized light and the subsequent transfer of their spin polarization to the localized spins of magnetic ions [4]. Therefore, diluted magnetic semiconductors based on II-VI materials, like (Cd,Mn)Te and (Zn,Mn)Se and their heterostructures, have been studied intensively [3,5–9]. Also, the carrier spin dynamics in DMS, being controlled by the strong s/p-d exchange interaction with the magnetic ions, is of great interest, for example, due to the resulting fast spin relaxation of electrons and holes on time scales of a few picoseconds [6–8,10]. Recently, the non-Markovian effects in the carrier spin dynamics in DMS have been considered theoretically [11,12].

In bulk CdTe, which has the sphalerite lattice structure, the measured hole spin relaxation times are short (a fraction of a picosecond) [4]. Any scattering of the hole momentum leads to the loss of spin orientation, as the spin-orbit interaction in the valence band is so strong that $\tau_p \approx \tau_s$, where τ_p and τ_s are the momentum relaxation time and the spin relaxation time, respectively. The rapid spin relaxation of nonequilibrium holes prohibits the observation of hole optical orientation in stationary-state experiments [4]. In the diluted magnetic semiconductor (Cd,Mn)Te, an additional mechanism is provided by the exchange scattering of the holes on magnetic ions, which should make the hole spin relaxation even faster.

The exchange interaction of carriers with magnetic ions in DMS results in formation of magnetic polarons (MP), which are typically composed of many localized spins oriented within the localization volume of a carrier or an exciton [13–16]. The spin dynamics of magnetic polarons is very

different from the dynamics of uncoupled carrier and localized spins. In wide band gap II-VI DMSs, like (Cd,Mn)Te, (Cd,Mn)Se, and (Zn,Mn)Se various types of magnetic polarons have been identified. Among them are: (i) the exciton magnetic polaron formed by a localized exciton, where the main contribution to the polaron binding energy comes from the hole exchange interaction, which exceeds the electron one by 4–5 times, (ii) the donor-bound magnetic polaron formed by an electron localized at a donor, (iii) the neutral acceptor-bound magnetic polaron (A^0-BMP) formed by a hole localized at an acceptor. Nonmagnetic localization of carriers and excitons is an important factor for the MP stability and its binding energy. In most cases the MP size is controlled by the nonmagnetic localization, e.g., the Bohr radius of an electron on a donor or a hole on an acceptor. In DMS quantum wells (QWs) carriers can also be localized within the fluctuation potential given, e.g., by the well width fluctuations. We showed recently that the localized resident holes in (Cd,Mn)Te/(Cd,Mn,Mg)Te QWs cause formation of hole magnetic polarons (HMP) [10]. In fact, the properties of the HMP should not differ from that of the A^0-BMP, both being controlled by the hole exchange with magnetic ions. The only difference expected comes from the reduction of the system symmetry going from the bulk to the QW case.

Information on magnetic polarons can be obtained using various optical methods: photoluminescence with selective excitation [16–18], time-resolved photoluminescence [16,19–21], and spin-flip Raman scattering [22–25]. Recently we showed that the spin relaxation dynamics of equilibrium hole magnetic polarons in DMS QWs can be studied by time-resolved pump-probe Kerr rotation [10].

Most of the results on MPs obtained so far were analyzed in the frame of the mean-field approach, which implies that the localized carrier (or exciton) is interacting with a large number of magnetic ions. This is valid when the Mn^{2+} concentration exceeds a few percent. In the very dilute regime, when the localized carrier interacts with only one (or a few) Mn^{2+} ions the mean-field approach is not valid anymore. We have
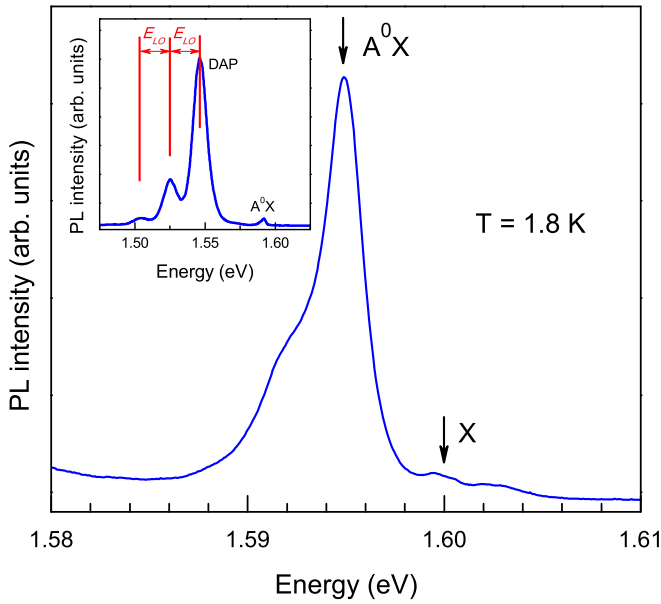
FIG. 1. Photoluminescence spectrum of $Cd_{1-x}Mn_xTe$ with $x = 0.005$ measured at $T = 1.8$ K. Inset shows the low energy part of the spectrum with DAP emission and the associated phonon replicas.

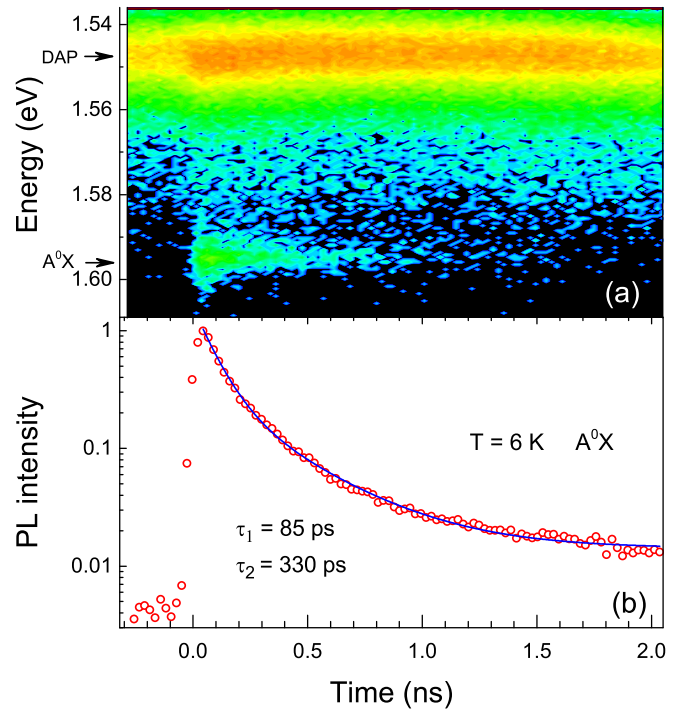
FIG. 2. Recombination dynamics of A^0X and DAPs. (a) Streak-camera image. (b) Recombination dynamics of acceptor-bound exciton (circles) detected at 1.595 eV and biexponential fit to the data (blue line). Laser photon energy 1.668 eV and $T = 6$ K.

investigated this case experimentally and theoretically for bulk $Cd_{1-x}Mn_xTe$ with $x = 0.005$ addressing the A^0-BMP by selective excitation of the donor-acceptor pair (DAP) states [17].

In this paper we study the spin dynamics of acceptor-bound hole magnetic polarons in bulk (Cd,Mn)Te with a low Mn concentration by time-resolved pump-probe Kerr rotation. The paper is organized as follows. Section II contains information about the studied sample and details of the experimental technique. In Sec. III the experimental results are presented. In Sec. IV a model of optical orientation of the hole magnetic polaron is discussed and compared with the experiment.

II. EXPERIMENTALS

The experiments were performed on a bulk $Cd_{1-x}Mn_xTe$ sample grown by the Bridgman technique and having a Mn concentration of $x = 0.005$. The crystal is nominally undoped, while due to the excess of Te or Cd vacancies as-grown crystals typically show p-type doping. The concentration of residual impurities (both donors and acceptors) is about 10^{16} cm^{-3}.

The photoluminescence (PL) spectrum measured under continuous-wave laser excitation with a photon energy of 2.34 eV at a temperature of $T = 1.8$ K is shown in Fig. 1. Its low energy part contains three intense broad bands separated by 20.5 meV (inset in Fig. 1), which corresponds to the LO-phonon energy in CdTe [26]. We associate the most intense line at 1.546 eV with recombination of donor-acceptor pairs (DAP) and the two other lines with the associated LO-phonon replicas. The two additional lines of weaker intensity in the high-energy part of the spectrum can be assigned to the acceptor-bound exciton A^0X (1.595 eV) and the free exciton X (1.600 eV) emission. More details on the PL spectrum of this sample can be found in Ref. [17].

The recombination dynamics of the acceptor-bound excitons A^0X and DAPs was measured by time-resolved PL and is shown in Fig. 2. The sample was excited by a Ti:Sapphire laser pulses (pulse duration 200 fs, repetition rate 76 MHz, photon energy 1.668 eV, excitation power $P_{ex} = 3.5$ W/cm^2). The emission was detected by a streak camera attached to a 0.5-m monochromator (time resolution of about 10 ps). One can see in Fig. 2(a) that the PL decay of the DAPs (the intense band) occurs on much longer time scales than the laser repetition period of 13.2 ns, as we conclude from the rather intensive signal observed at negative delay times, i.e., at delays of about 13 ns. This is in accordance with the long recombination times reported for DAPs in other papers [9]. The A^0X recombination dynamics [weaker line at the bottom of Fig. 2(a)] is shown in Fig. 2(b). A fit to the experimental data with a biexponential decay gives us recombination times of $\tau_1 = 85$ ps and $\tau_2 = 330$ ps. Due to the low intensity of the free exciton line it was not possible to measure its recombination dynamics. Since in the PL spectrum under continuous-wave excitation (Fig. 1) the A^0X intensity exceeds the intensity of the free exciton, the capture probability of the exciton on the acceptor obviously exceeds the probability of its recombination. Therefore, one can conclude that the free exciton lifetime does not exceed the A^0X lifetime. Note that the dynamic spectral shift of the PL lines to low energies, which is typical for the magnetic polaron formation, is not detected here. This can be explained by the fact that in the studied sample with a low Mn concentration, the magnetic polaron shift is small. In this case the A^0-BMP cannot be identified by the spectral shift of the emission maximum but
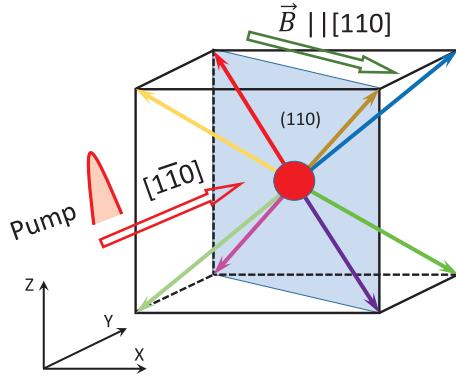
FIG. 3. Experimental scheme and crystal orientation. The blue plane is the cleaved surface (110) of our sample. The red open arrow gives the direction of the exciting light [1$\bar{1}$0]. The green open arrow shows the direction of the external magnetic field. The other colored arrows specify the direction of the easy magnetization axis {111} as described in the text. The axes shown in the figure are the crystallographic axes.

through the asymmetric tail of the resonantly excited DAP [17]. Moreover, the magnetic polaron formation time exceeds the exciton lifetime [17].

The time-resolved pump-probe Kerr rotation (KR) technique [1,10,27,28] is used to study the spin dynamics. Pulses with duration of 1.5 ps were emitted by a Ti:Sapphire laser with a repetition period of $T_R = 13.2$ ns. An elasto-optical modulator switches the circular polarization of the excitation between σ^+ and σ^- with a frequency of 50 kHz. The laser photon energy was tuned within the spectral range from the free exciton to the DAP. The probe pulses were linearly polarized and their Kerr rotation was measured by a balanced photoreceiver using a lock-in amplifier. The excitation density of the pump pulses, P_{pump}, was varied from 0.8 to 16 W/cm^2.

The Faraday or Kerr rotation pump-probe technique has several advantages for investigation of the spin dynamics in DMS, compared to photoluminescence. Among them are: (1) the PL detection is limited by the recombination time of the studied states, which restricts the temporal range of the studied spin dynamics, and (2) as we have demonstrated in Ref. [10] pump-probe KR allows one to obtain information about equilibrium magnetic polarons, e.g., hole magnetic polarons formed by resident holes.

The sample was placed in a cryostat and its temperature was varied from $T = 1.7$ to 25 K. The surface of the cleaved sample coincides with the crystallographic plane (110), see Fig. 3. The sample was oriented such that the vector of the external magnetic field **B** was lying in the plane of the surface. The direction of the excitation light beam was perpendicular to this surface (that is along the direction [1$\bar{1}$0]) (Voigt geometry).

III. EXPERIMENTAL RESULTS

The pump-probe KR signal measured at 1.6007 eV (near the exciton resonance) in a magnetic field of 0.5 T is shown in Fig. 4(a) and for different magnetic fields in Fig. 4(b). The signal has a complicated shape and consists of three components:
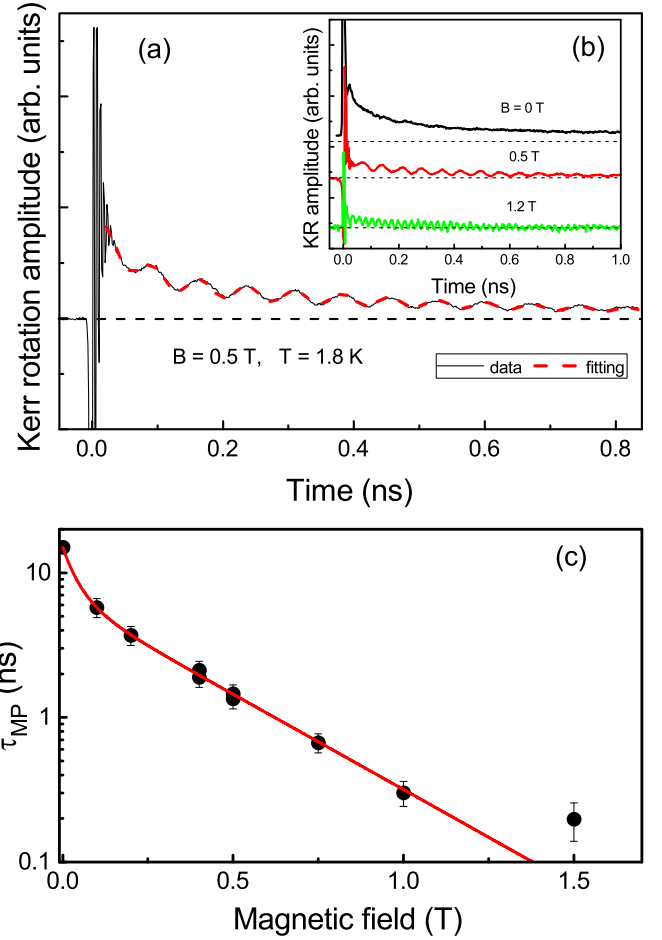

FIG. 4. (a) KR signal (black line) measured at 1.6007 eV. $B = 0.5$ T, $T = 1.8$ K, and $P_{pump} = 1$ W/cm^2. Red dashed line is fit for time delays longer than 25 ps using Eq. (1). The fitting parameters are $T_{2,Mn}^* = 540$ ps and $\tau_{MP} = 1.1$ ns. (b) KR signals measured for different magnetic field strengths. Data are shifted vertically for clarity. Dotted lines indicate zero level. (c) Decay time of the long-lived nonoscillating component as a function of magnetic field. Red line is a fit to the data using Eqs. (1) and (17) from Ref. [10].

(i) a rapidly oscillating component during the first 20 ps, (ii) a component oscillating at much lower frequency during times up to 1 ns, and (iii) a long-lived nonoscillating component.

In order to extract the dephasing or decay times, the relative amplitudes and the precession Larmor frequencies of these components, the spin beat signals were fitted with the following function:

$$K(t) = A \exp\left(-\frac{t}{T_{2,e}^*}\right)\cos(2\pi\omega_e t + \phi)$$

$$+ B \exp\left(-\frac{t}{T_{2,Mn}^*}\right)\cos(2\pi\omega_{Mn}t + \psi)$$

$$+ C \exp\left(-\frac{t}{\tau_{MP}}\right). \quad (1)$$

Here A (B), $T_{2,e}^*$ ($T_{2,Mn}^*$), ω_e (ω_{Mn}), and ϕ (ψ) are the amplitude, dephasing time, Larmor precession frequency, and initial phase of the fast (slow) oscillating component of the
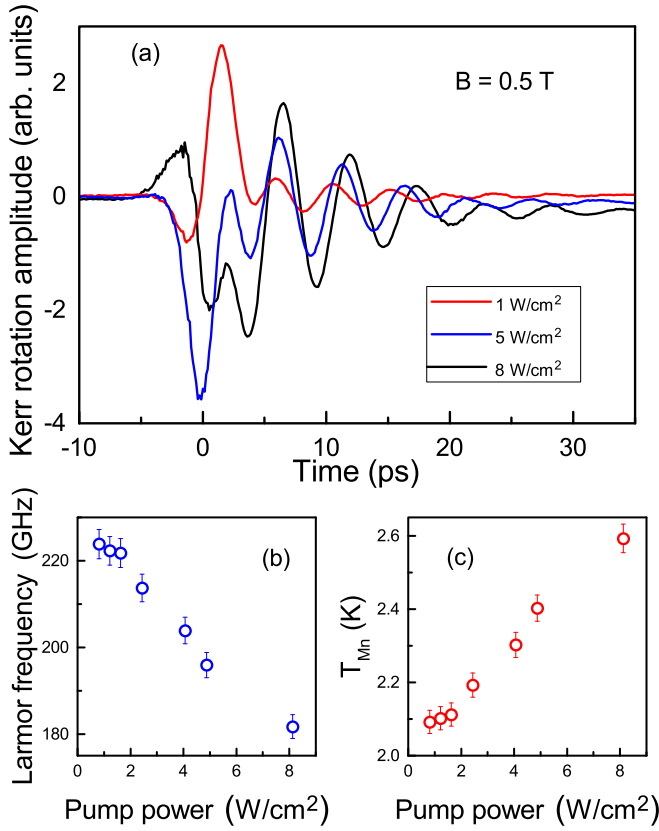
FIG. 5. (a) KR signals of photogenerated electrons at different pump powers. (b) Dependence of electron Larmor precession frequency on pump power. (c) Evaluated Mn spin temperature at different pump powers. Laser photon energy is 1.6028 eV, $B = 0.5$ T, and $T = 1.8$ K.
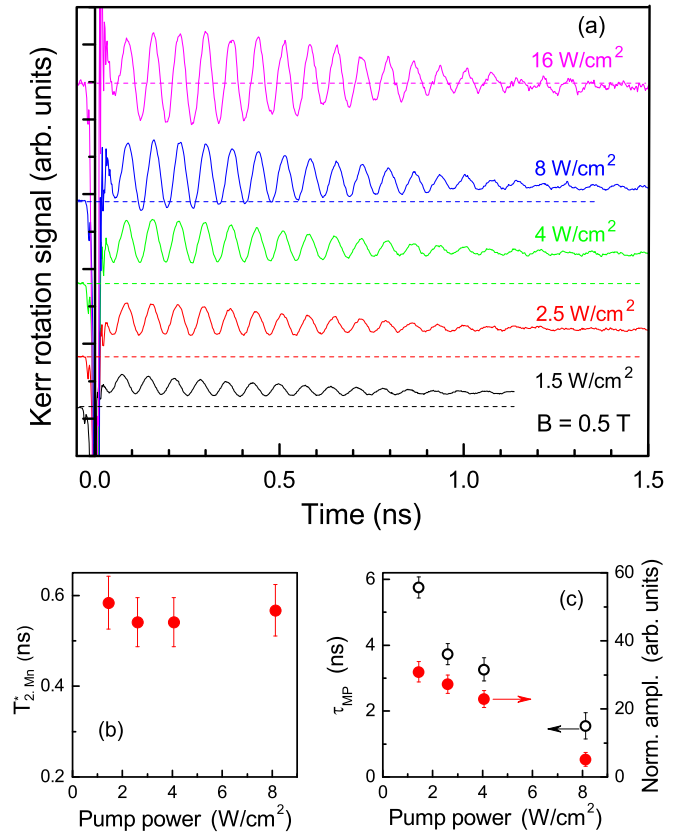

FIG. 6. (a) KR signals of Mn spins at different pump powers. Data are shifted vertically for clarity. Dashed lines indicate zero level. (b) Dependence of Mn spin dephasing time $T_{2,\mathrm{Mn}}^*$ on pump power. (c) Pump power dependencies for the nonoscillating component: decay time τ_{MP} and amplitude normalized to the pump power. Laser photon energy is 1.6028 eV, $B = 0.5$ T, and $T = 1.8$ K.

KR signal. C and τ_{MP} are the amplitude and the decay time of the nonoscillating component, respectively.

The rapidly oscillating component is shown in more detail in Fig. 5(a). It is related to the Larmor precession of the photogenerated electron spins with an effective g factor $g^* \simeq 32$ and a spin dephasing time of $T_{2,e}^* \simeq 10$ ps. The large g^* is due to the exchange interaction of the electrons with the Mn spins. The frequency of the electron Larmor precession depends on the excitation power and decreases with increasing power [Fig. 5(b)]. The reason for that is apparently the heating of the manganese spin system by photogenerated carriers, which results in a decrease of the Mn polarization and of the giant Zeeman splitting of the electrons [29]. From the period of the electron Larmor precession we estimate the Mn spin temperatures T_{Mn} given in Fig. 5(c) and the actual concentration of manganese in the sample to be 0.005 using equations from Ref. [29].

In addition to the short-lived and rapidly oscillating component the KR signal contains a relatively slowly oscillating component corresponding to a g factor of 2 and a spin dephasing time $T_{2,\mathrm{Mn}}^* = 540$ ps at $B = 0.5$ T [Fig. 6(a)] which we attribute to the Larmor precession of Mn^{2+} spins [1,6,7,17]. It should be noted that the dephasing time of Mn spins does not depend on the pump power [Fig. 6(b)]. This can be explained

by the influence of the hyperfine interaction on the dynamics of the Mn^{2+} spins, as it was demonstrated in Ref. [30].

Also a nonoscillating component with large amplitude and long decay time is observed in the KR signal [Fig. 4(a)]. A fitting to the experimental data for delay times longer than 25 ps using Eq. (1) is shown by the red dashed line. The amplitude and decay time of the nonoscillating component (τ_{MP}) depend on the laser photon energy, magnetic field, temperature, and pump power. This long-lived nonoscillating component is observed only for the laser energy in resonance with the exciton transition but becomes negligibly small when the laser is detuned from the exciton. At $B = 0$ T the long relaxation time in the KR signal is about 15 ns [Fig. 4(b)] and decreases with increasing magnetic field dropping to 200 ps at 1.5 T [Fig. 4(c)]. A fitting of the dependence $\tau_{MP}(B)$ using Eqs. (1) and (17) from Ref. [10] gives the following parameters: $B_{ex} = 0.16$ T, $g_\perp / g_{z'z'} = 0.19$, and $d\Delta E_z^{\mathrm{hh}}/dB = 4.9$ meV/T. Here ΔE_z^{hh} is Zeeman splitting of heavy hole states. The KR signal amplitude also decreases with increasing magnetic field [Fig. 4(b)]. One can see from the results presented in Fig. 7 that a rather small increase in temperature from 1.7 to 7 K is sufficient to suppress the nonoscillating component. The decay time τ_{MP} and amplitude normalized to the pump power depend on the pump power [Fig. 6(c)].
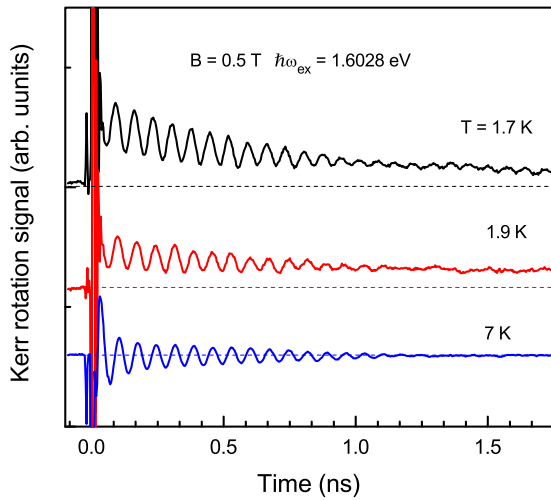
FIG. 7. KR signal at different temperatures. Data are shifted vertically for clarity. Dashed lines indicate zero level. Laser photon energy is 1.6028 eV and $P_{pump} = 5$ W/cm^2.

At pump powers exceeding 10 W/cm^2 the nonoscillating component disappears. It is important to note that long-lived signal persists at times long after the exciton recombination.

The sensitivity of the pump-probe KR setup is mainly determined by two factors: (i) the efficiency of optical orientation of the magnetic polarons, which also depends on the absorption coefficient, and (ii) the efficiency of KR signal detection. When the coherent spin dynamics of the exciton is studied, it is optimal to set the laser photon energy at the exciton energy. For investigation of the acceptor-bound hole magnetic polaron the detection would be optimal at the A^0X energy, but many more spin-oriented excitons can be excited at the exciton energy, which then are captured on the acceptors with only partial loss of their spin orientation. As a result, the optimal laser photon energy for investigating the magnetic polaron dynamics is between the exciton and the A^0X energies.

IV. MODEL CONSIDERATIONS

We turn now to the origin of the nonoscillating KR signal. Its experimental signatures are very similar to those measured for (Cd,Mn)Te-based QW structures, where we identified the corresponding signal as the contribution from the equilibrium hole magnetic polaron formed from resident holes localized on QW width fluctuations [10]. There are two key experimental features. (i) Absence of oscillations in the KR amplitude in a magnetic field, which means that the orientation of the spin polarization is stabilized and fixed by some mechanism. In the QW case the mechanism is provided by a strong anisotropy of the hole g factor, whose in-plane component is close to zero. (ii) Strong magnetic field dependence of the decay time τ_{MP} with a short initial part. This is related to the fact that the spin relaxation of the hole magnetic polaron in the QW requires a flipping polaron moment between two stationary states with orientations parallel to the quantization axis. They are separated by a barrier $E_a(B)$, which depends on the magnetic field strength. As a result $\tau_{MP}(B, T) \approx \tau_0 \exp[E_a(B)/k_BT]$, where

$E_a(0) = -E_{MP}$, τ_0 is a prefactor and k_B is the Boltzmann constant.

As we observe both of these experimental signatures also in the bulk (Cd,Mn)Te sample, it is reasonable to assume that the nonoscillating signal in bulk is caused by hole magnetic polarons. But in this case the resident hole is localized on an acceptor. It is less obvious, however, that the hole spin in a bulk cubic crystal is anisotropic, which is essential for the considered mechanism. It is worthwhile to recall that the acceptor-bound magnetic polarons have been studied in (Cd,Mn)Se crystals with wurtzite structure and strong crystal anisotropy, which results in a bistable polaron behavior [31–33]. From the symmetry point of view the case of bulk crystals with wurtzite structure is quite similar to the case of quantum well structures [10,34]. Below we will discuss possible mechanisms for the hole spin anisotropy in bulk cubic DMS crystals, comment on the optical orientation mechanism, and evaluate parameters of the A^0-BMP.

A. Mechanisms of hole MP anisotropy in bulk DMS

We can suggest two possible mechanisms of the MP anisotropy in a bulk crystal.

(i) It has been shown theoretically and experimentally that due to the spin-orbit interaction in the valence band of (Cd,Mn)Te the hole magnetic polaron becomes anisotropic, i.e., has a preferential direction of its magnetic moment (the so-called cubic anisotropy) [35,36]. Namely, the directions {111} are easy magnetization axes in (Cd,Mn)Te and the magnetic polarons are aligned along them, see colored arrows in Fig. 3. In thermal equilibrium and at zero external magnetic field the magnetic moments of the A^0-BMPs are directed equally along all {111} directions and the average polarization of the MP ensemble is zero. However, an external magnetic field or circularly polarized excitation can induce a net polarization in the ensemble of MPs.

(ii) The second scenario leading to the anisotropy of the A^0-BMP is the following. As noted above, the Mn concentration in our sample is very small. For acceptors with a Bohr radius $a_B = 1$ nm and $x = 0.005$, the concentration of magnetic ions $N_{Mn} = xN_0 = 7 \times 10^{-19}$ cm^{-3} (N_0 is the concentration of cations) and the parameter $\frac{4}{3}\pi a_B^3 N_0 x = 0.3$, i.e., statistically there is less than one Mn ion in the hole localization volume at an acceptor. As was shown in Ref. [17], in this case the dominant combination to the A^0-BMP energy comes from the hole exchange interaction with the Mn ion that is located nearest to the acceptor. The spherical Coulomb potential of the acceptor localizing the hole will be changed owing to the exchange interaction between the hole and the nearest Mn (the spherical potential of the acceptor acquires a uniaxial distortion). The axis of this anisotropy is the direction from the acceptor to the nearest manganese ion. As Mn in the (Cd,Mn)Te lattice substitutes Cd and the Cd vacancy serves as an acceptor, the nearest to an acceptor Mn ions are positioned along the following directions: (a) [110], the distance from the acceptor is $a/\sqrt{2}$ (a is the lattice constant), (b) [100], distance from the acceptor is a, (c) [121], the distance from the acceptor is $a\sqrt{3}/2$.

B. Mechanism of optical orientation of A^0-BMP

We suggest the following mechanism for the optical orientation of the A^0-BMPs resulting in observation of their long-lived spin dynamics. Circularly polarized pump light generates spin oriented excitons, followed by their spin selective capture to A^0 acceptors which leads to the formation of A^0X. This induces an imbalance in the system of A^0 bound magnetic polarons, i.e., a net polarization of these polarons appears. As one can see in Fig. 1, the A^0X line in the PL spectrum is much more intense than the free exciton line. This means that after photogeneration an exciton is quickly captured by a neutral acceptor A^0, forming A^0X bound exciton. We assume that during the fast capture process the hole spin in the exciton does not change its orientation (if the hole would have lost its orientation, we could not have seen optical orientation).

As we mentioned above, the A^0-BMPs are oriented along the anisotropy axes that coincide with the local anisotropy axes for holes bound to acceptors (A^0-holes). This means that the hole angular momentum projections for the specific magnetic polaron are $|\uparrow\rangle$ and $|\downarrow\rangle$. Here, the notations $|\uparrow\rangle$ and $|\downarrow\rangle$ correspond to the hole angular momentum projections parallel and opposite to the anisotropy axes z'. The anisotropy axes z' are inclined relative to the z axis at some angle θ, so that the hole state $J_z = +3/2$ (z is the direction of the excitation light) can be represented in the reference frame related to the direction of the specific polaron magnetic moment by $|+3/2\rangle = a_1 |\uparrow\rangle + a_2 |\downarrow\rangle$, where $a_1 = \cos\theta/2$ and $a_2 = \sin\theta/2$. Circularly polarized (say σ^+) light pulses excite excitons with angular momentum $|+1\rangle = |+3/2, -1/2\rangle$ (in the notations $|S_z\rangle = |j_z, s_z\rangle$, where S_z, j_z, and s_z are the projections of the exciton, hole, and electron spins). This exciton is captured by an acceptor $A^0 |\downarrow\rangle$ with probability a_1^2 and by $A^0 |\uparrow\rangle$ with probability a_2^2. As $a_1^2 \geqslant a_2^2$ for σ^+ excitation this process will result in orientation of the A^0X excitons. The net spin orientation of this complex is determined by the spin of the uncompensated electron because the total angular momentum of the two holes in the A^0X complex is equal to zero. The fast oscillations in the KR signal are just a manifestation of the A^0X electron precession in a transversal magnetic field, see Fig. 4(a).

Since the exciton capture is a spin selective process (the total spin of the holes in the ground state of the A^0X complex is equal to zero, as it has two holes in a singlet state), the excitons $|+1\rangle = |+3/2, -1/2\rangle$ are trapped preferentially by neutral acceptors with hole spin projection $|-3/2\rangle$. As a consequence, the hole exchange field acting on the Mn ions in the A^0-BMP is switched off by the exciton capture. The exchange field of an electron that appears in this case is much smaller (due to the smaller exchange constant and the larger localization volume), therefore, we neglect it. Also, the exciton capture on an acceptor leads to additional energy that dissipates in the Mn spin system within the acceptor vicinity destroying the Mn spin polarization, i.e., destroying A^0-BMP. In contrast, the majority of acceptors with hole spin projection $|+3/2\rangle$ remain unperturbed as the excitons are not captured by them. The KR dynamics allows us to study the spin relaxation of these unperturbed magnetic polarons.

For relaxation of the induced net polarization of the MPs it is necessary to overcome the barrier given by the anisotropy. The consequences of that are a significant increase of the relaxation time τ_{MP} and an absence of magnetization precession in a transverse magnetic field [10].

To explain qualitatively the magnetic field dependence of τ_{MP}, we should take into account that the relaxation of the magnetization, i.e., the reorientation of the A^0-BMP magnetic moment between $A^0 |\downarrow\rangle$ and $A^0 |\uparrow\rangle$ occurs through the saddle point, namely through the x direction. As a transverse magnetic field B_x induces a Mn magnetic moment M_x, the barrier between the two stable polaron states $A^0 |\downarrow\rangle$ and $A^0 |\uparrow\rangle$ decreases and as a consequence τ_{MP} decreases. It is worth mentioning and discussing an interesting peculiarity of our observation, namely the qualitative and quantitative similarity of the $\tau_{MP}(B)$ dependencies in QWs [10] and bulk (Cd,Mn)Te.

C. Evaluation of A^0-BMP parameters

The model approach for the hole MP was developed in Ref. [10] for a (Cd,Mn)Te-based QW with a strong anisotropy of the hole g factor. We suggest that this model can be used also to analyze the experimental results for the A^0-BMP in bulk (Cd,Mn)Te because the main ingredients of the model—the anisotropy of the hole g factor and the value of the MP energy—are similar for both cases. As we will show below, the evaluation of the MP parameters for the studied bulk (Cd,Mn)Te sample gives reasonable values.

For the QW, the parameters evaluated from the experimental dependence of $\tau_{MP}(B)$ were: exchange field $B_{ex} = 0.05$ T and hole g factor anisotropy parameter $g_\perp/g_{zz} = 0.04$. Here g_{zz} is the hole g factor along the QW growth axis and $g_\perp$ is the in-plane hole g factor. That gives for the energy of the hole MP a value of $E_{MP} = 0.5$ meV [10]. By applying this model approach to the experimental results in the present paper, the following parameters are obtained for the A^0-BMP in bulk from fitting the $\tau_{MP}(B)$ dependence in Fig. 4(c). We obtain $B_{ex} = 0.16$ T, $g_\perp/g_{z'z'} = 0.19$, and $d\Delta E_z^{hh}/dB = 4.9$ meV/T. Using these parameters we evaluate the energy of magnetic polaron $E_{MP} = \frac{1}{2}(d\Delta E_z^{hh}/dB)B_{ex} = 0.4$ meV. The larger value of B_{ex} in the bulk sample compared to the QW is apparently due to the stronger localization of the hole wave function on the acceptor. The larger value of $g_\perp/g_{z'z'}$ in bulk can be attributed to the smaller anisotropy in the bulk sample. An estimate of the parameter $d\Delta E_z^{hh}/dB$ can be obtained using the measured value of the $g_e^* = 32$ factor for the electron. Although we could not measure the g factor for a hole, it is known [3] that the exchange constant for a hole is four times larger than that of an electron. Therefore, $g_h^* = 4g_e^*$ and $d\Delta E_z^{hh}/dB = \mu_B g_h^* = 7.4$ meV/T. This value is close to what we obtained from the fitting of experimental data.

From fitting experimental data we get parameter $g_\perp/g_{z'z'} = 0.19$, which does not necessarily means such a strong g factor anisotropy of the hole, but evidences that the hole magnetic polaron energy depends on the orientation of the hole spin in respect of the crystallographic axis and the difference in HMP energy can reach five times. It has been shown in Ref. [36] that the anisotropy of the hole effective masses can be responsible for that. Using this approach in Ref. [34] it has been estimated that the HMP energy for [111] orientation of the hole spin may
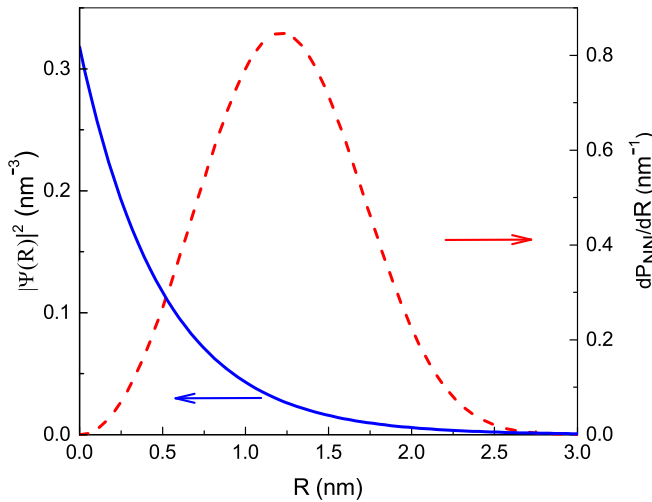
FIG. 8. Square of wave function of the hole localized at an acceptor and probability for the acceptor to have a nearest Mn at distance R.

exceed by 2.7 times the one for [100] orientation, which is in reasonably good agreement with our experimental data.

It is worth noting that in (Cd,Mn)Te with a low concentration of Mn and a small acceptor Bohr radius, the A^0-BMP energy is spread across a wide energy range. This dispersion of the A^0-BMP energy depends on the distribution of Mn spins in the acceptor vicinity and can be described by the Poisson statistics. This is the case when the contribution of the Mn ion nearest to the acceptor center to the magnetic polaron energy is dominant [17]. Here we take an acceptor wave function in the form $\psi(R) = \frac{1}{\sqrt{\pi a_B^3}} \exp(-R/a_B)$ and the probability for the acceptor to have a nearest Mn at distance R is given by:

$$\frac{dP_{NN}}{dR} = 4\pi R^2 x N_0 \exp\left(-\frac{4\pi R^3 x N_0}{3}\right). \qquad (2)$$

Figure 8 shows the probability for the acceptor to have a nearest Mn at distance R (red line) and the density of probability of hole localized on acceptor (blue line) as a function of R. The distribution of a number of acceptors to have a nearest Mn at distance R has its maximum at $R_{\max} = 1.2$

nm, where the acceptor hole density ($|\psi(R)|^2$) is small (as is the hole exchange field B_{ex}). The value $B_{ex} = 0.16$ T can be attributed to the hole exchange field B_{ex} at the maximum of the distribution of the number of acceptors as a function of R.

Measurements of the KR signal performed in a magnetic field oriented at different angles in the sample plane (110) did not reveal any additional features of the magnetic polaron (the polaron amplitude and dephasing time practically did not change). Therefore, we conclude that we cannot distinguish experimentally between the two scenarios for the A^0-BMP anisotropy discussed above.

V. CONCLUSIONS

We have reported the observation of optical orientation of equilibrium hole magnetic polarons involving holes bound to acceptors in a bulk (Cd,Mn)Te sample with a small concentration of manganese. The main parameters of the acceptor-bound hole magnetic polaron have been determined. It is important to note that the oscillating component related to the coherent spin dynamics of the Mn spins and the long-lived nonoscillating component related to the A^0-BMPs have different origins. The oscillating component is induced by the spin transfer to the Mn spins from the photogenerated carriers, while the long-lived nonoscillating component is due to optical orientation of the A^0-BMP. In the latter case the anisotropy of the A^0-BMP leads to the absence of oscillations in transversal magnetic field and the long decay of the MP spin polarization. Despite the fact that we used a theoretical model [10] developed for QWs, it describes sufficiently well the experimental results for bulk (Cd,Mn)Te and gives reasonable parameters of A^0-BMP.

[1] D. D. Awschalom, D. Loss, and N. Samarth (eds.), *Semiconductor Spintronics and Quantum Computation* (Springer-Verlag, Berlin, 2002).

[2] G. Slavcheva and P. Roussignol (eds.), *Optical Generation and Control of Quantum Coherence in Semiconductor Nanostructures* (Springer, Berlin, 2010).

[3] J. Kossut and J. A. Gaj (eds.), *Introduction to the Physics of Diluted Magnetic Semiconductors* (Springer, Berlin, 2010).

[4] F. Meier and B. P. Zakharchenya (eds.), *Optical Orientation* (North-Holland, New York, 1984).

[5] J. Stühler, G. Schaack, M. Dahl, A. Waag, G. Landwehr, K. V. Kavokin, and I. A. Merkulov, Multiple Mn^{2+}-Spin-Flip Raman Scattering at High Fields via Magnetic Polaron States in Semimagnetic Quantum Wells, Phys. Rev. Lett. **74**, 2567 (1995).

[6] S. A. Crooker, J. J. Baumberg, F. Flack, N. Samarth, and D. D. Awschalom, Terahertz Spin Precession and Coherent Transfer of Angular Momenta in Magnetic Quantum Wells, Phys. Rev. Lett. **77**, 2814 (1996).

[7] S. A. Crooker, D. D. Awschalom, J. J. Baumberg, F. Flack, and N. Samarth, Optical spin resonance and transverse spin relaxation in magnetic semiconductor quantum wells, Phys. Rev. B **56**, 7574 (1997).

[8] R. Akimoto, K. Ando, F. Sasaki, S. Kobayashi, and T. Tani, Larmor precession of Mn^{2+} moments initiated by the exchange field of photoinjected carriers in CdTe/(Cd, Mn)Te quantum wells, Phys. Rev. B **57**, 7208 (1998).

[9] Tran Hong Nhung, R. Planel, C. Benoit a la Guillaume, and A. K. Bhattacharjee, Acceptor-bound magnetic polaron in $Cd_{1-x}Mn_xTe$ semimagnetic semiconductors, Phys. Rev. B **31**, 2388 (1985).

[10] E. A. Zhukov, Yu. G. Kusrayev, K. V. Kavokin, D. R. Yakovlev, J. Debus, A. Schwan, I. A. Akimov, G. Karczewski, T. Wojtowicz, J. Kossut, and M. Bayer, Optical orientation of hole magnetic polarons in (Cd, Mn)Te/(Cd, Mn, Mg)Te quantum wells, Phys. Rev. B **93**, 245305 (2016).

[11] M. Cygorek, P. I. Tamborenea, and V. M. Axt, Nonperturbative correlation effects in diluted magnetic semiconductors, Phys. Rev. B **93**, 035206 (2016).

[12] M. Cygorek, F. Ungar, P. I. Tamborenea, and V. M. Axt, Influence of nonmagnetic impurity scattering on spin dynamics in diluted magnetic semiconductors, Phys. Rev. B **95**, 045204 (2017).

[13] P. G. De Gennes, Effects of double exchange in magnetic crystals, Phys. Rev. **118**, 141 (1960).

[14] M. A. Krivoglaz and A. A. Trushchenko, Current carriers in ferromagnetic semiconductors. A case of strong interaction, Sov. Phys. Solid State **11**, 2531 (1970) [Fiz. Tverd. Tela **11**, 3119 (1969)].

[15] E. L. Nagaev, Self-trapped states of charge carriers in magnetic semiconductors, J. Magn. Magn. Mater. **110**, 39 (1992).

[16] D. R. Yakovlev and W. Ossau, Magnetic polarons, in *Introduction to the Physics of Diluted Magnetic Semiconductors*, edited by J. Kossut and J. A. Gaj (Springer, Berlin, 2010), Chap. 7, pp. 221–262.

[17] Yu. G. Kusrayev, K. V. Kavokin, G. V. Astakhov, W. Ossau, and L. W. Molenkamp, Bound magnetic polarons in the very dilute regime, Phys. Rev. B **77**, 085205 (2008).

[18] W. D. Rice, W. Liu, V. Pinchetti, D. R. Yakovlev, V. I. Klimov, and S. A. Crooker, Direct measurements of magnetic polarons in $Cd_{1-x}Mn_xSe$ nanocrystals from resonant photoluminescence, Nano Lett. **17**, 3068 (2017).

[19] G. Mackh, W. Ossau, D. R. Yakovlev, A. Waag, G. Landwehr, R. Hellmann, and E. O. Göbel, Localized exciton magnetic polarons in $Cd_{1-x}Mn_xTe$, Phys. Rev. B **49**, 10248 (1994).

[20] H. D. Nelson, L. R. Bradshaw, Ch. J. Barrows, V. A. Vlaskin, and D. R. Gamelin, Picosecond dynamics of excitonic magnetic polarons in colloidal diffusion-doped $Cd_{1-x}Mn_xSe$ quantum dots, ACS Nano **9**, 11 (2015).

[21] R. Beaulac, L. Schneider, P. I. Archer, G. Bacher, and D. R. Gamelin, Light-induced spontaneous magnetization in doped colloidal quantum dots, Science **325**, 973 (2009).

[22] E. D. Isaacs, D. Heiman, M. J. Graf, B. B. Goldberg, R. Kershaw, D. Ridley, K. Dwight, A. Wold, J. Furdyna, and J. S. Brooks, Bound magnetic polarons below $T = 1$ K, Phys. Rev. B **37**, 7108 (1988).

[23] T. Dietl and J. Spalek, Effect of Fluctuations of Magnetization on the Bound Magnetic Polaron: Comparison with Experiment, Phys. Rev. Lett. **48**, 355 (1982).

[24] D. Heiman, P. A. Wolff, and J. Warnock, Spin-flip Raman scattering, bound magnetic polaron, and fluctuations in (Cd, Mn)Se, Phys. Rev. B **27**, 4848 (1983).

[25] R. Planel, Tran Hong Nhung, G. Fishman, and M. Nawrocki, Magnetic fluctuation observation in donor-bound magnetic polarons, J. Phys. (France) **45**, 1071 (1984).

[26] D. J. Olego, P. M. Raccah, and J. P. Faurie, Compositional dependence of the Raman frequencies and line shapes of $Cd_{1-x}Zn_xTe$ determined with films grown by molecular-beam epitaxy, Phys. Rev. B **33**, 3819 (1986).

[27] J. M. Kikkawa and D. D. Awschalom, Resonant Spin Amplification in n-Type GaAs, Phys. Rev. Lett. **80**, 4313 (1998).

[28] E. A. Zhukov, D. R. Yakovlev, M. Bayer, M. M. Glazov, E. L. Ivchenko, G. Karczewski, T. Wojtowicz, and J. Kossut, Spin coherence of a two-dimensional electron gas induced by resonant excitation of trions and excitons in CdTe/(Cd, Mg)Te quantum wells, Phys. Rev. B **76**, 205310 (2007).

[29] D. R. Yakovlev and I. A. Merkulov, Spin and energy transfer between carriers, magnetic ions, and lattice, in *Introduction to the Physics of Diluted Magnetic Semiconductors*, edited by J. Kossut and J. A. Gaj (Springer, Berlin, 2010), Chap. 8, pp. 263–303.

[30] S. Cronenberger, M. Vladimirova, S. V. Andreev, M. B. Lifshits, and D. Scalbert, Optical Pump-Probe Detection of Manganese Hyperfine Beats in (Cd, Mn)Te Crystals, Phys. Rev. Lett. **110**, 077403 (2013).

[31] D. Scalbert, M. Nawrocki, C. Benoit a la Guillaume, and J. Cernogora, Anisotropy of magnetic polarons bound to acceptors in $Cd_{1-x}Mn_xSe$, Phys. Rev. B **33**, 4418 (1986).

[32] A. K. Bhattacharjee, Crystal-field model for acceptor-associated bound magnetic polarons in wurtzite semiconductors, Phys. Rev. B **35**, 9108 (1987).

[33] D. Scalbert, J. Cernogora, and C. Benoit a la Guillaume, Bistability of magnetic polarons bound to acceptors in a wurtzite semimagnetic semiconductor, Phys. Rev. B **38**, 13246 (1988).

[34] R. Fiederling, D. R. Yakovlev, W. Ossau, and G. Landwehr, Exciton magnetic polarons in (100)- and (120)-oriented semimagnetic digital alloys (Cd, Mn)Te, Phys. Rev. B **58**, 4785 (1998).

[35] A. V. Kudinov, Yu. G. Kusraev, B. P. Zakharchenya, and V. N. Yakimovich, Anisotropy of cubic semimagnetic $Cd_{1-x}Mn_xTe$ solid solutions and excitonic magnetic polaron energy from polarized-luminescence measurements, Fiz. Tverd. Tela (St. Petersburg) **40**, 894 (1998) [Sov. Phys. Solid State **40**, 823 (1998)].

[36] T. L. Linnik, Yu. G. Rubo, and V. I. Sheka, Anisotropy of a hole magnetic polaron in a semimagnetic semiconductor, Pis'ma Zh. Eksp. Teor. Fiz. **63**, 209 (1996) [Sov. Phys. JETP Lett. **63**, 222 (1996)].